REPORT 1344

A SIMPLIFIED METHOD FOR APPROXIMATING THE TRANSIENT MOTION IN ANGLES OF ATTACK AND SIDESLIP DURING A CONSTANT ROLLING MANEUVER[1]

By LEONARD STERNFIELD

SUMMARY

The transient motion in angles of attack and sideslip during a constant rolling maneuver has been analyzed. Simplified expressions are presented for the determination of the pertinent modes of motion as well as the modal coefficient corresponding to each mode.

Calculations made with and without the derivatives C_{Y_β} (side force due to sideslip) and C_{L_α} (lift-curve slope) indicate that although these derivatives increase the total damping of the system they do not markedly affect the transient motion.

INTRODUCTION

Recent flight tests of airplanes designed with their mass concentrated primarily in the fuselage have indicated that during a rolling maneuver the airplane experiences large uncontrollable motions in angles of attack and sideslip. A fundamental analysis of this pitch-yaw divergence problem, in which the rolling velocity of the airplane is assumed constant, is presented in reference 1. This analysis, concerned primarily with the stability of the system, makes possible the calculation of the divergence boundaries and the prediction of the range of rolling velocities for which the airplane motions will diverge. Analog studies made at the National Advisory Committee for Aeronautics for several research airplanes have indicated that reference 1 is a helpful guide in a roll-coupling investigation, but detailed-motion studies based on five degrees of freedom and with pilot inputs taken into account are essential to the analysis. Also, calculated time histories of the airplane motion indicate that large angles of attack and sideslip which are objectionable to a pilot and which may induce severe loads on the airplane may be encountered for constant rolling velocities outside the critical range.

The purpose of this paper is to extend the analysis of reference 1 by analyzing the transient motion in angles of attack and sideslip. Simplified expressions are presented which permit an accurate and rapid estimate of the maximum angles of attack and sideslip for an airplane rolling at a constant velocity which should apply to the case of an airplane entering a rolling maneuver up to the point of recovery from the maneuver. The airplane is assumed to be initially disturbed by an input in the side-force equation equal to the product of the rolling velocity and trim angle of attack. A comparison is made of the time histories obtained by using the simplified and exact expressions (obtained from the four degrees of freedom assuming constant rolling velocity) for a currently designed swept-wing fighter flying at a Mach number of 0.7 at an altitude of 32,000 feet.

SYMBOLS

b	wing span, ft
$\bar{c}$	wing mean aerodynamic chord, ft
C_L	lift coefficient, $\frac{\text{Lift}}{qS}$
C_l	rolling-moment coefficient, $\frac{\text{Rolling moment}}{qSb}$
C_m	pitching-moment coefficient, $\frac{\text{Pitching moment}}{qS\bar{c}}$
C_n	yawing-moment coefficient, $\frac{\text{Yawing moment}}{qSb}$
C_Y	side-force coefficient, $\frac{\text{Side force}}{qS}$
I_X	moment of inertia of airplane about principal X-axis, slug-ft^2
I_Y	moment of inertia of airplane about principal Y-axis, slug-ft^2
I_Z	moment of inertia of airplane about principal Z-axis, slug-ft^2
M_X	rolling moment, ft-lb
m	airplane mass, slugs
P	period, sec
p	rolling velocity, radians/sec
p_0	steady rolling velocity, radians/sec
q	pitching velocity, radians/sec; dynamic pressure, lb/sq ft
r	yawing velocity, radians/sec
S	wing area, sq ft
t	time, sec
$T_{1/2}$	time to damp to one-half amplitude, sec
T_2	time to double amplitude, sec
V	airplane velocity, ft/sec
α_0	initial angle of attack of airplane principal axis, radians
$\Delta\alpha$	incremental change in angle of attack, radians
$\alpha=\alpha_0+\Delta\alpha$	
β	angle of sideslip, radians
λ	root of characteristic equation
$a\pm ib$	complex roots of characteristic equation
λ_1,λ_2	real roots of characteristic equation

[1] Supersedes recently declassified NACA Research Memorandum L56F04 by Leonard Sternfield, 1956

$$\omega_\psi^2=\frac{C_{n_\beta}qSb}{I_Zp_0^2}$$

$$\omega_\vartheta^2=\frac{-C_{m_\alpha}qS\bar{c}}{I_Yp_0^2}$$

$$C_{m_\alpha}=\frac{\partial C_m}{\partial\alpha}$$

$$C_{n_\beta}=\frac{\partial C_n}{\partial\beta}$$

$$C_{L_\alpha}=\frac{\partial C_L}{\partial\alpha}$$

$$C_{l_p}=\frac{\partial C_l}{\partial\frac{pb}{2V}}$$

$$C_{m_q}=\frac{\partial C_m}{\partial\frac{q\bar{c}}{2V}}$$

$$C_{n_r}=\frac{\partial C_n}{\partial\frac{rb}{2V}}$$

$$C_{Y_\beta}=\frac{\partial C_Y}{\partial\beta}$$

$$L_\alpha=qSC_{L_\alpha}$$

$$M_\alpha=qS\bar{c}C_{m_\alpha}$$

$$M_q=\frac{qS\bar{c}^2}{2V}C_{m_q}$$

$$N_\beta=qSbC_{n_\beta}$$

$$N_r=\frac{qSb^2}{2V}C_{n_r}$$

$$Y_\beta=qSC_{Y_\beta}$$

EQUATIONS OF MOTION

In this analysis, on the assumption of constant forward velocity and constant rolling velocity, the following linearized equations of motion of an airplane referred to the principal axes were used:

Pitching:

$$\dot{q}-\left(\frac{I_Z-I_X}{I_Y}\right)p_0r=\frac{M_qq}{I_Y}+\frac{M_\alpha}{I_Y}\Delta\alpha \tag{1a}$$

Yawing:

$$\dot{r}-\left(\frac{I_X-I_Y}{I_Z}\right)p_0q=\frac{N_r}{I_Z}r+\frac{N_\beta}{I_Z}\beta \tag{1b}$$

Side force:

$$\dot{\beta}+r-p_0\Delta\alpha=\frac{Y_\beta}{mV}\beta+p_0\alpha_0 \tag{1c}$$

Normal force:

$$\dot{\alpha}-q+p_0\beta=-\frac{L_\alpha}{mV}\Delta\alpha \tag{1d}$$

When the substitutions $q=q_0e^{\lambda t}$, $r=r_0e^{\lambda t}$, $\beta=\beta_0e^{\lambda t}$, and $\Delta\alpha=(\Delta\alpha)_0e^{\lambda t}$ are used in the equations written in determinant form, λ must be a root of the stability equation

$$A\lambda^4+B\lambda^3+C\lambda^2+D\lambda+E=0 \tag{2}$$

where

$$A=1$$

$$B=-\frac{N_r}{I_Z}-\frac{M_q}{I_Y}-\frac{Y_\beta}{mV}+\frac{L_\alpha}{mV}$$

$$C=-\left(\frac{I_X-I_Y}{I_Z}\right)\left(\frac{I_Z-I_X}{I_Y}\right)p_0^2-\frac{M_\alpha}{I_Y}+\frac{N_\beta}{I_Z}+\frac{M_q}{I_Y}\frac{N_r}{I_Z}+p_0^2+\frac{Y_\beta}{mV}\frac{N_r}{I_Z}+\frac{Y_\beta}{mV}\frac{M_q}{I_Y}-\frac{L_\alpha}{mV}\frac{N_r}{I_Z}-\frac{L_\alpha}{mV}\frac{M_q}{I_Y}-\frac{L_\alpha}{mV}\frac{Y_\beta}{mV}$$

$$D=-\left(\frac{N_r}{I_Z}+\frac{M_q}{I_Y}\right)p_0^2-\frac{M_q}{I_Y}\frac{N_\beta}{I_Z}+\frac{M_\alpha}{I_Y}\frac{N_r}{I_Z}-\frac{M_q}{I_Y}\frac{N_r}{I_Z}\frac{Y_\beta}{mV}+\frac{M_q}{I_Y}\frac{N_r}{I_Z}\frac{L_\alpha}{mV}+\frac{N_\beta}{I_Z}\frac{L_\alpha}{mV}+\frac{M_\alpha}{I_Y}\frac{Y_\beta}{mV}+\frac{L_\alpha}{mV}\frac{Y_\beta}{mV}\frac{N_r}{I_Z}+\frac{L_\alpha}{mV}\frac{Y_\beta}{mV}\frac{M_q}{I_Y}+\frac{Y_\beta}{mV}\left(\frac{I_X-I_Y}{I_Z}\right)\left(\frac{I_Z-I_X}{I_Y}\right)p_0^2-\frac{L_\alpha}{mV}\left(\frac{I_X-I_Y}{I_Z}\right)\left(\frac{I_Z-I_X}{I_Y}\right)p_0^2$$

and

$$E=-\left(\frac{I_X-I_Y}{I_Z}\right)\left(\frac{I_Z-I_X}{I_Y}\right)p_0^4-\frac{M_\alpha}{I_Y}\left(\frac{I_X-I_Y}{I_Z}\right)p_0^2-\frac{N_\beta}{I_Z}\left(\frac{I_Z-I_X}{I_Y}\right)p_0^2+\frac{M_q}{I_Y}\frac{N_r}{I_Z}p_0^2-\frac{M_\alpha}{I_Y}\frac{N_\beta}{I_Z}-\frac{M_q}{I_Y}\frac{N_\beta}{I_Z}\frac{L_\alpha}{mV}-\frac{M_\alpha}{I_Y}\frac{N_r}{I_Z}\frac{Y_\beta}{mV}-\frac{M_q}{I_Y}\frac{N_r}{I_Z}\frac{L_\alpha}{mV}\frac{Y_\beta}{mV}+\frac{L_\alpha}{mV}\frac{Y_\beta}{mV}\left(\frac{I_X-I_Y}{I_Z}\right)\left(\frac{I_Z-I_X}{I_Y}\right)p_0^2$$

In reference 1, C_{L_α} and C_{Y_β} were assumed to be equal to zero; this assumption is representative of the condition in which the center of gravity is moving in a straight line. In this analysis the case where $C_{L_\alpha}=C_{Y_\beta}=0$ (referred to as case (a)) is considered, as well as the case where the values of C_{L_α} and C_{Y_β} are finite (referred to as case (b)).

ANALYSIS AND DISCUSSION

DIVERGENCE BOUNDARIES

The conditions necessary for the system described by equations (1) to be stable are that the coefficients of the characteristic equation (eq. (2)) must be positive and that Routh's discriminant, $BCD-AD^2-B^2E$, must be greater than zero. From an examination of the characteristic equation of this system, it can be shown that, for aircraft designed with positive static stability and for conditions where each of the damping derivatives C_{n_r}, C_{m_q}, C_{L_α}, and C_{Y_β} adds damping to the system, the oscillatory modes will be stable for all values of the steady rolling velocity. Thus, the only type of instability that could be encountered is an aperiodic mode which occurs when the constant term of the characteristic equation, the E coefficient, is negative. As shown in reference 1, divergence boundaries, obtained by setting $E=0$,

can be plotted as a function of the squares of the natural frequencies in pitch and yaw nondimensionalized to the square of the rolling velocity, ω_θ^2 and ω_ψ^2, respectively. These divergence boundaries are shown in figure 1 for cases (a) and (b) for an airplane whose mass and aerodynamic characteristics are presented in table I. The nondimensional pitch and yaw frequencies of the airplane described in table I fall along the straight line, with the slope equal to $\frac{-C_{m_\alpha}}{C_{n_\beta}} \frac{I_Z}{I_Y} \frac{\bar{c}}{b}$, shown in figure 1. Each point on this line corresponds to a particular value of p_0 and, as p_0 increases, the point moves along the line toward the origin. For case (a), the airplane line intersects the divergence boundaries at two points and thus defines the critical range of rolling velocities where a divergent mode exists, namely, $1.86 < |p_0| < 2.33$. For case (b) the airplane line lies in the stable region and the motion is therefore stable for all values of p_0.

TABLE I

MASS AND AERODYNAMIC CHARACTERISTICS OF AIRPLANE

m, slugs	745
I_X, slug-ft^2	10, 976
I_Y, slug-ft^2	57, 100
I_Z, slug-ft^2	64, 975
C_{n_r}, per radian	−0. 095
C_{m_q}, per radian	−3. 5
C_{m_α}, per radian	−0. 36
C_{n_β}, per radian	0. 057
C_{Y_β}, per radian	−0. 28
C_{L_α}, per radian	3. 85
C_{l_p}, per radian	−0. 255
V, ft/sec	691
S, sq ft	377
$\bar{c}$, ft	11. 3
b, ft	36. 6
q, lb/sq ft	197

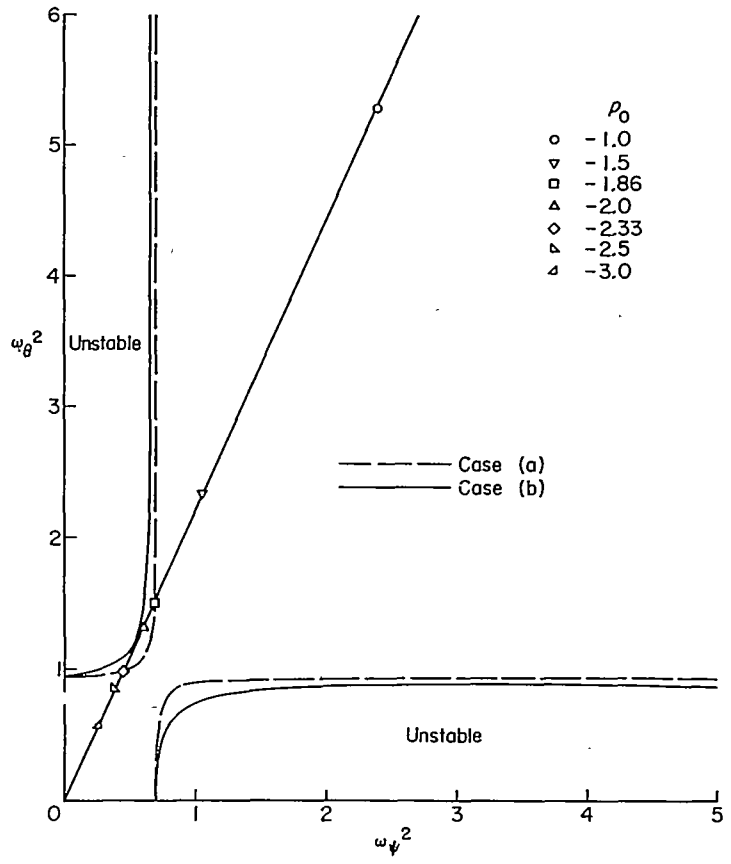

FIGURE 1.—Boundaries in the ω_θ^2, ω_ψ^2 plane which define regions of aperiodic divergence for example airplane.

CHARACTERISTIC MODES

The roots of the characteristic stability equation corresponding to the absolute values of p_0 shown in figure 1 are presented in tables II (a) and II (b) for cases (a) and (b),

TABLE II

ROOTS OF THE CHARACTERISTIC EQUATION FOR VALUES OF p_0 SHOWN IN FIGURE 1

(a) Roots for case (a)

p_0	Exact		Approximate	
0	−0. 210±2. 29i	−0. 0526±1. 54i		
−1. 0	−0. 156±2. 90i	−0. 107±0. 922i	−0. 152±3. 06i	−0. 111±0. 874i
−1. 5	−0. 143±3. 34i	−0. 12 ±0. 464i	−0. 144±3. 39i	−0. 119±0. 457i
−1. 86	−0. 137±3. 66i	−0. 251 0	−0. 133±3. 67i	−0. 25 0
−2. 0	−0. 135±3. 79i	−0. 355+0. 0996	−0. 136±3. 79	−0. 354+0. 0997
−2. 33	−0. 131±4. 09i	−0. 256 0	−0. 132±4. 10i	−0. 252 0
−2. 5	−0. 129±4. 24i	−0. 134±0. 267i	−0. 130±4. 26i	−0. 133±0. 294i
−3. 0	−0. 124±4. 70i	−0. 139±0. 768i	−0. 125±4. 77i	−0. 138±0. 756i

(b) Roots for case (b)

p_0	Exact		Approximate	
0	−0. 488±2. 30i	−0. 0729±1. 54i		
−1. 0	−0. 362±2. 89i	−0. 199 ±0. 942i	−0. 352±3. 10i	−0. 209±0. 876i
−1. 5	−0. 337±3. 33i	−0. 224 ±0. 483i	−0. 340±3. 42i	−0. 221±0. 469i
−1. 86	−0. 327±3. 66i	−0. 322 −0. 145	−0. 332±3. 71i	−0. 311−0. 146
−2. 0	−0. 324±3. 79i	−0. 453 −0. 020	−0. 329±3. 83i	−0. 444−0. 020
−2. 33	−0. 318±4. 08i	−0. 374 −0. 111	−0. 322±4. 13i	−0. 363−0. 113
−2. 5	−0. 316±4. 24i	−0. 245 ±0. 258i	−0. 320±4. 29i	−0. 241±0. 255i
−3. 0	−0. 311±4. 70i	−0. 250 ±0. 760i	−0. 312±4. 80i	−0. 248±0. 743i

respectively. A method of approximating the roots of the characteristic equation is presented in the appendix. The roots for $p_0=0$ which correspond to the condition where no coupling exists between the lateral and longitudinal modes are also given in the table. If the roots are complex, $\lambda=a\pm i\omega$, $P=\frac{2\pi}{\omega}$, and $T_{1/2}=\frac{-0.693}{a}$; whereas, for a real root λ_1, $T_{1/2}=\frac{-0.693}{\lambda_1}$ or $T_2=\frac{0.693}{\lambda_1}$.

The roots for $p_0=0$, for both cases (a) and (b), indicate that the motion consists of two independent oscillatory modes, a longitudinal and lateral oscillation with periods of 2.74 seconds and 4.08 seconds, respectively. The damping of the oscillation for case (b) is greater than that for case (a) because the damping derivatives C_{Y_β} and C_{L_α} were assumed equal to zero in case (a). The values of $T_{1/2}$ in seconds are given in the following table:

Case	$T_{1/2}$	
	Longitudinal oscillation	Lateral oscillation
(a)	3.3	13.2
(b)	1.4	9.5

For values of $|p_0|$ other than zero, the lateral variables β and r are coupled with the longitudinal variables α and q and the system now has the characteristic modes shown in table II for each of the variables β, r, α, and q. It should be noted that as $|p_0|$ increases, the frequency of the high frequency mode continues to increase and the damping decreases. However, the frequency of the other oscillation decreases until $|p_0|$ reaches approximately 1.86 when the oscillation breaks down into two aperiodic modes. In case (a) at this value of $|p_0|$, a zero root is obtained and the unstable region begins. The system remains unstable, with one aperiodic divergent mode, until $|p_0|$ becomes equal to 2.33. In case (b), the system is stable although two aperiodic modes occur for $1.86<|p_0|<2.33$. For $|p_0|>2.33$, the oscillation reappears in cases (a) and (b) and the frequency and damping increase as $|p_0|$ increases.

From the contour lines of constant oscillation frequencies presented in reference 1, it appears that, in general, the frequency of one of the oscillatory modes will always decrease and probably break down into two aperiodic modes as $|p_0|$ increases.

MOTIONS IN $\beta(t)$ AND $\Delta\alpha(t)$

Time histories were calculated by the method of Laplace transform (ref. 2) of the motions in β and $\Delta\alpha$ for the several values of p_0 shown in figure 1. The disturbance acting on the airplane is represented by the term $p_0\alpha_0$ in the side-force equation while the airplane is rolling in a negative direction. The motions in $\frac{\beta(t)}{\alpha_0}$ and $\frac{\Delta\alpha(t)}{\alpha_0}$ are presented in figures 2 and 3 for cases (a) and (b), respectively. A comparison of figures 2 and 3 shows that the inclusion of C_{L_α} and C_{Y_β} modifies

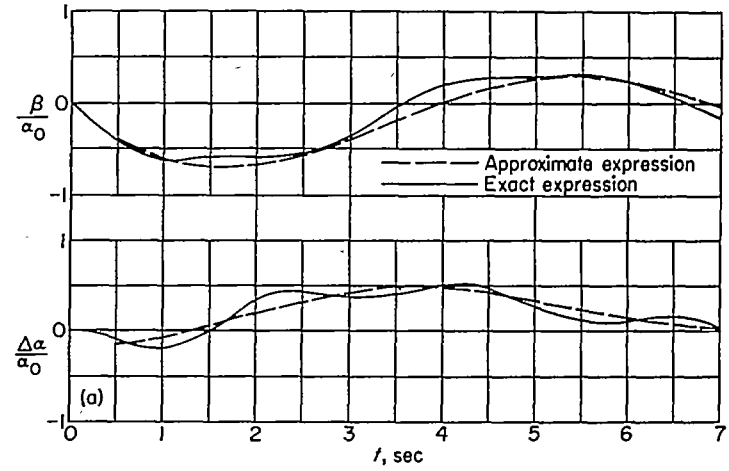

(a) $p_0=-1.0$.

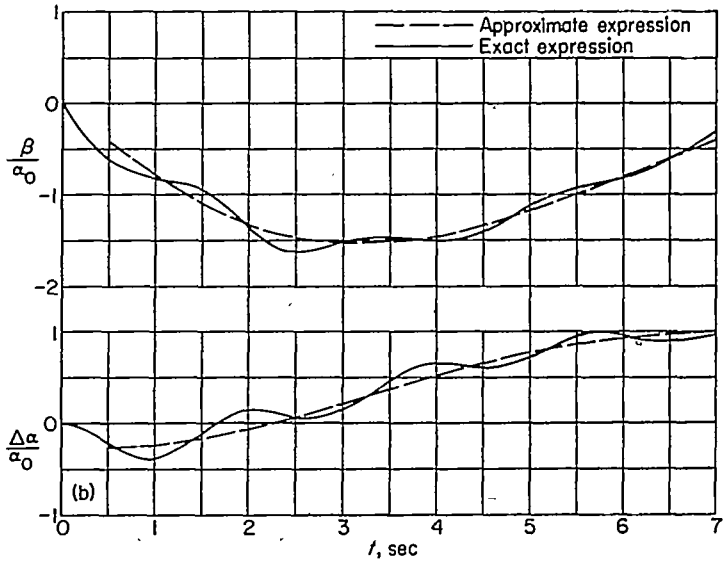

(b) $p_0=-1.5$.

FIGURE 2.—Time histories of β/α_0 and $\Delta\alpha/\alpha_0$ for case (a).

the motions slightly. Additional time histories were made and are presented in figure 4 for the same airplane but with the following assumed values of the derivatives: $C_{m_\alpha}=-0.09$, $C_{n_\beta}=0.114$, and $C_{Y_\beta}=C_{L_\alpha}=0$. For $p_0=-1.0$, the airplane would be located in figure 1 at the point $\omega_\theta^2=1.32$ and $\omega_\psi^2=4.77$.

Although the modes of motion involved in the transient behavior of the airplane will be stable for points along the airplane line located in the stable region, that is, $2.33<|p_0|<1.86$ in case (a) and for all values of $|p_0|$ in case (b), the magnitudes of $\Delta\alpha$ and β developed during the transient motion may be large enough to cause severe loads on the airplane. For example, in the particular flight condition for which the motions were calculated, where $\alpha_0=5°$, the airplane develops a sideslip angle of about $-8°$ at $p_0=-1.5$ and $\Delta\alpha$ is about $-20°$ at $p_0=-3.0$. These values are reached in about 3 seconds.

In all the motions the high-frequency mode is clearly evident, although the amplitude of this mode is relatively small. Hence, the high-frequency mode modifies the shape of the motion only slightly. Thus, for $p_0=-1.0$, -1.5, -2.5,

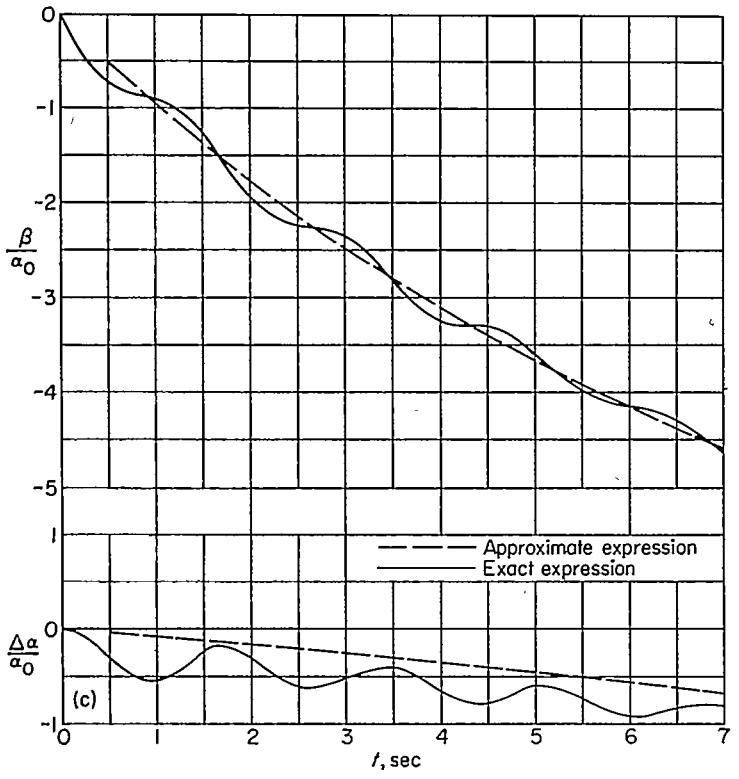

(c) $p_0=-1.86$.

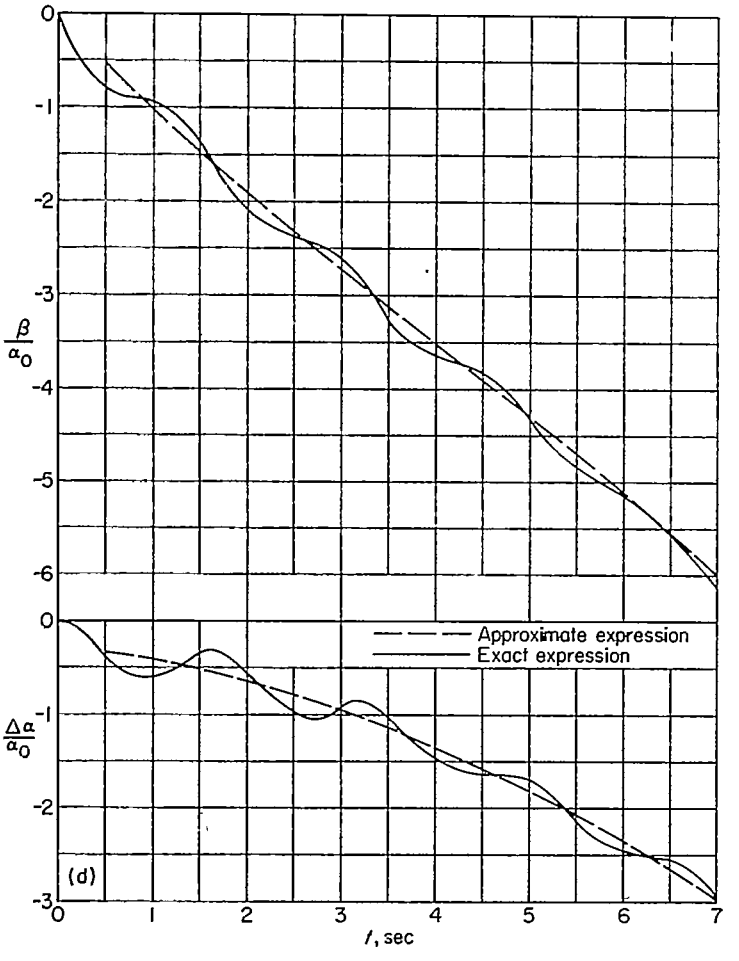

(d) $p_0=-2.0$.

FIGURE 2.—Continued.

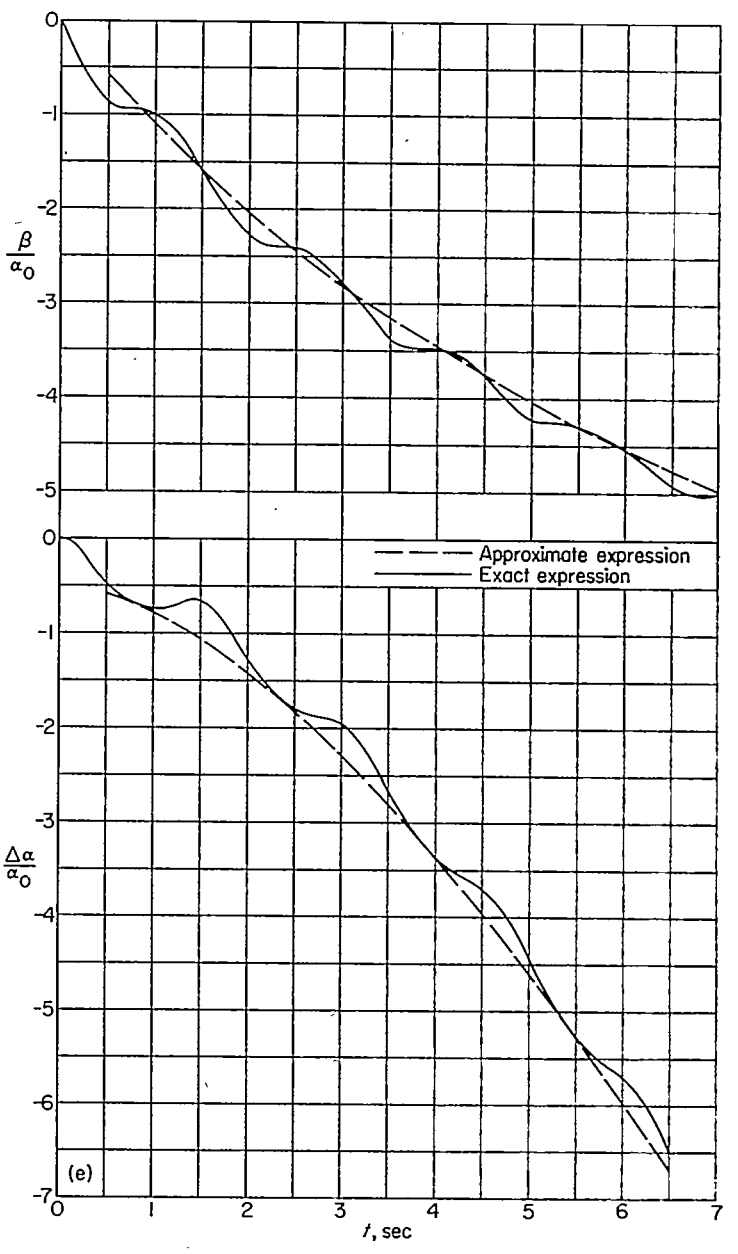

(e) $p_0=-2.33$.

FIGURE 2.—Continued.

and -3.0, the low-frequency mode is of primary importance in the motions, whereas for $p_0=-1.86$, -2.0, and -2.33, the aperiodic modes are of primary importance. In addition, the analytical expressions for the motions would also contain a constant term which represents the steady-state value of β and $\Delta\alpha$ if the system is stable. A good approximation to the time history could therefore be expressed in general form for $p_0=-1.0$, -1.5, -2.5, and -3.0 as

$$\frac{\beta(t)}{\alpha_0} \text{ or } \frac{\Delta\alpha(t)}{\alpha_0}=K_0+K_1e^{at}\sin(\omega t+\epsilon) \tag{3}$$

For case (b) when $p_0=-1.86$, -2.0, and -2.33 and for case (a) when $p_0=-2.0$, the following equation is obtained:

$$\frac{\beta(t)}{\alpha_0} \text{ or } \frac{\Delta\alpha(t)}{\alpha_0}=K_0+K_2e^{\lambda_1 t}+K_3e^{\lambda_2 t} \tag{4}$$

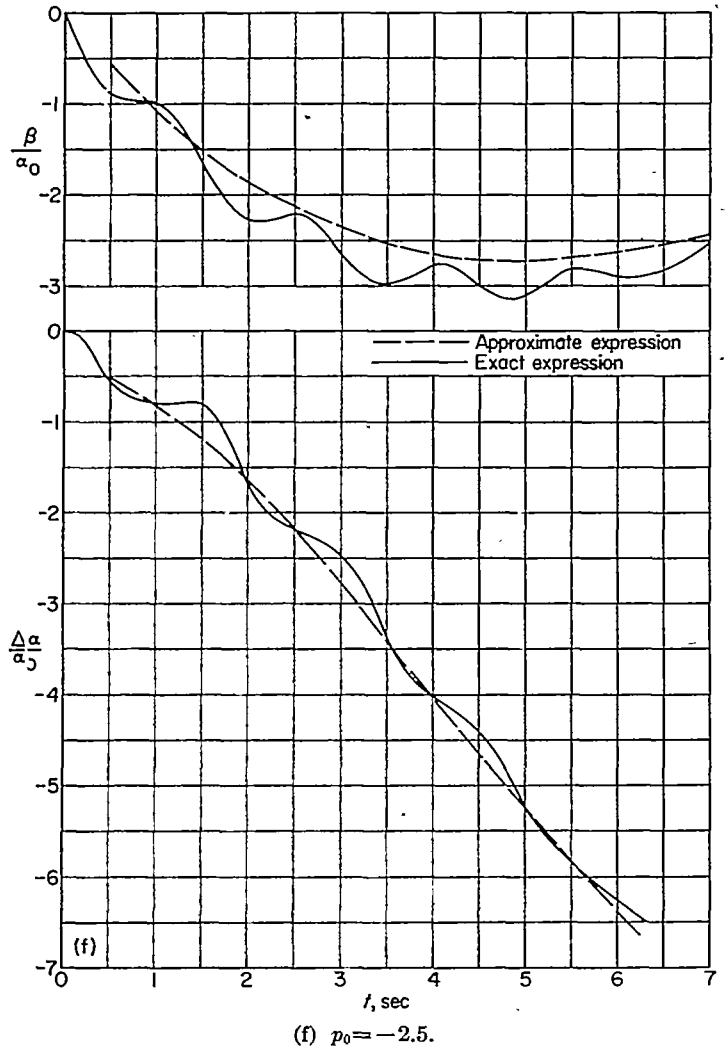

(f) $p_0 = -2.5$.

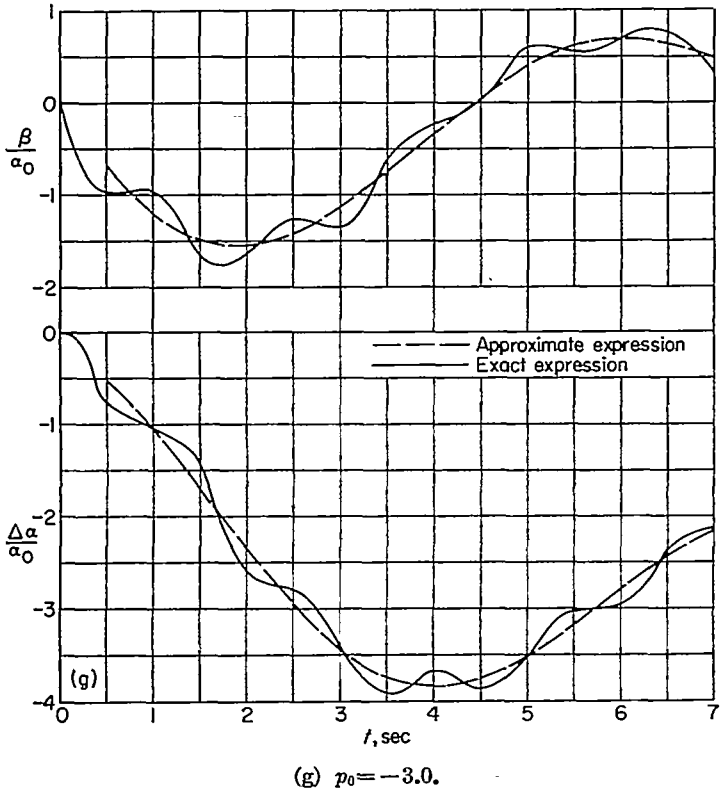

(g) $p_0 = -3.0$.

FIGURE 2.—Concluded.

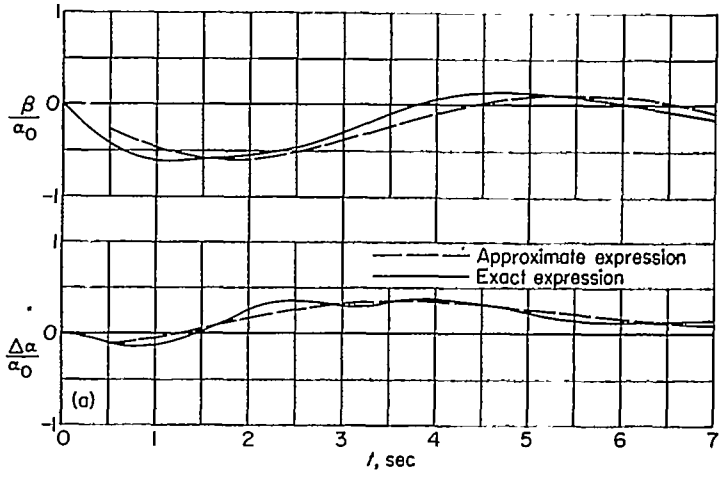

(a) $p_0 = -1.0$.

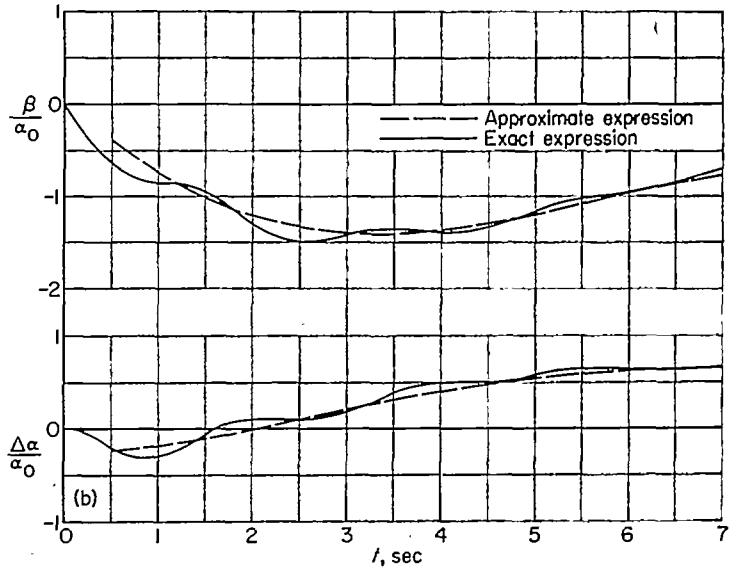

(b) $p_0 = -1.5$.

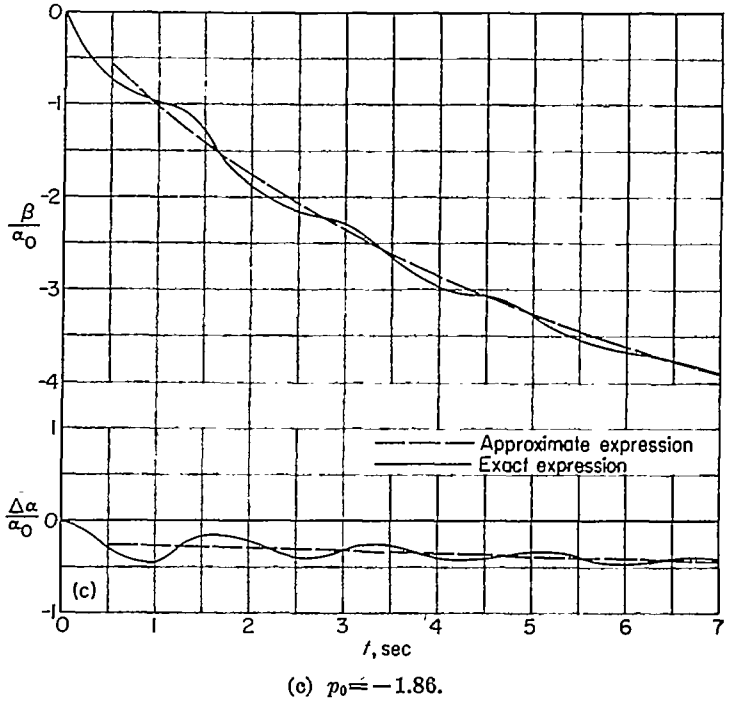

(c) $p_0 = -1.86$.

FIGURE 3.—Time histories of β/α_0 and $\Delta\alpha/\alpha_0$ for case (b).

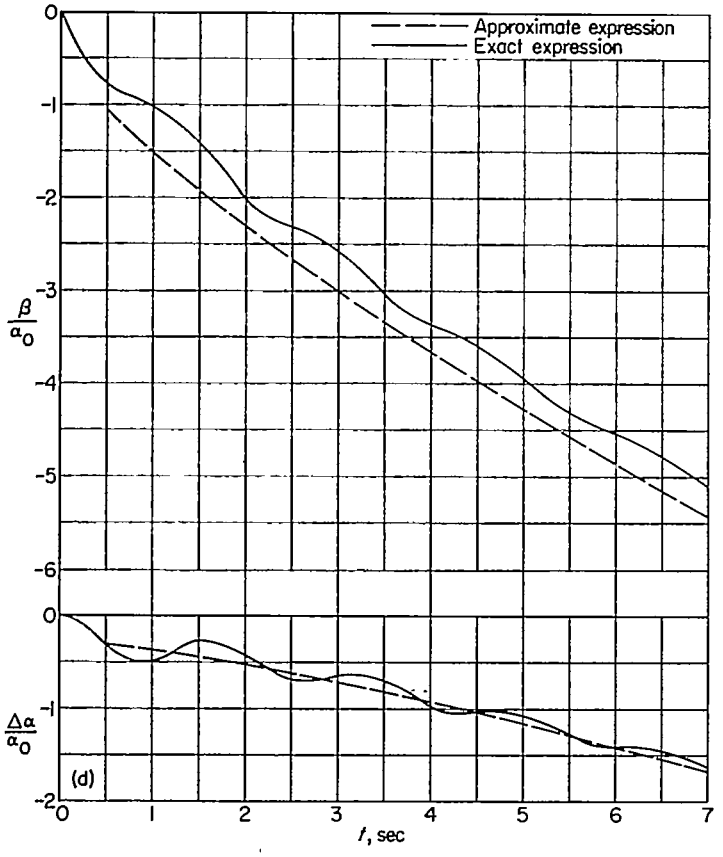

(d) $p_0=-2.0$.

FIGURE 3.—Continued.

and for case (a) when $p_0=-1.86$ and -2.33,

$$\frac{\beta(t)}{\alpha_0} \text{ or } \frac{\Delta\alpha(t)}{\alpha_0}=K_4t+K_5(e^{\lambda t}-1) \tag{5}$$

Since the high-frequency mode is omitted from expressions (3), (4), and (5), the values of $\frac{\beta(t)}{\alpha_0}$ and $\frac{\Delta\alpha(t)}{\alpha_0}$ will not satisfy the initial condition of being zero at $t=0$.

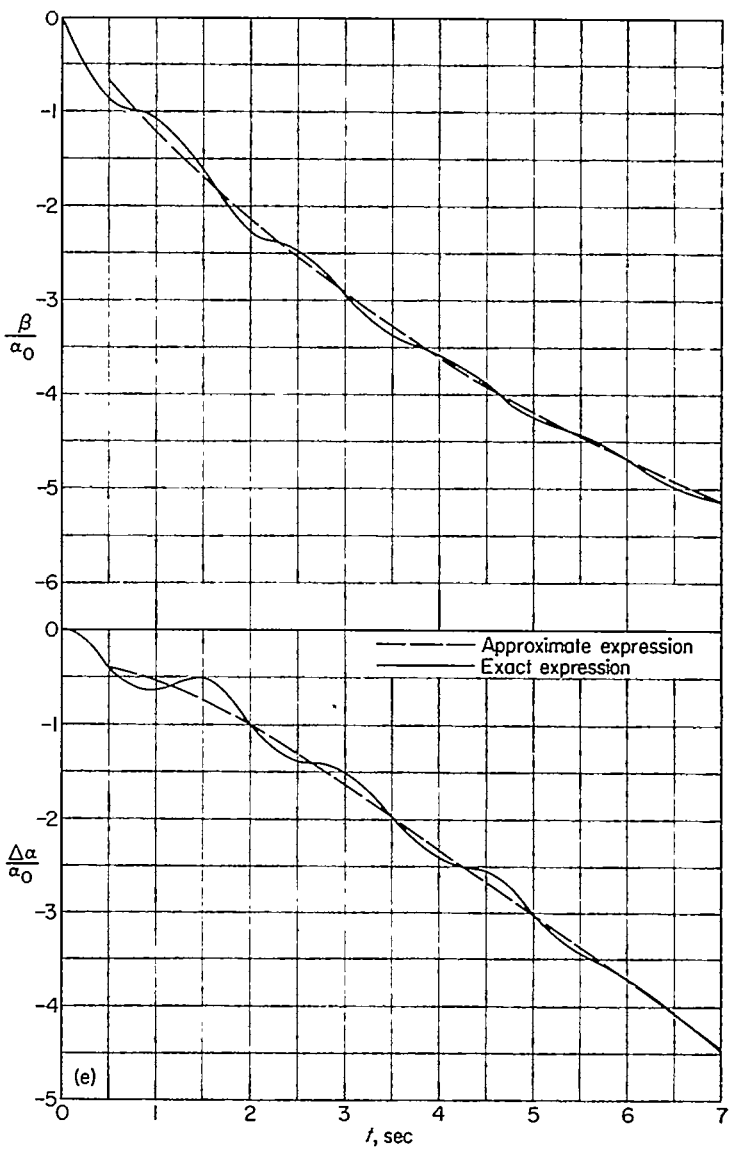

(e) $p_0=-2.33$.

FIGURE 3.—Continued.

By differentiating expressions (3), (4), and (5) and setting them equal to zero, the maximum values of β and $\Delta\alpha$ and the time at which they occur could be easily determined. In these calculations, β and $\Delta\alpha$ occurred at about ¼ and ½ of the period, respectively.

APPROXIMATION OF THE AMPLITUDE COEFFICIENTS AND PHASE ANGLE

The amplitude coefficients K_0, K_1, K_2, K_3, K_4, and K_5 and the phase angle ϵ in expressions (3), (4), and (5) can be calculated directly by using the Heaviside expansion formula given on page 45 of reference 2. A detailed examination of the exact expressions for the amplitude coefficients and phase angle indicated that many of the terms appearing in the expressions had a negligible effect on the resultant magnitudes. Thus the following simplified expressions were derived which result in good agreement with the exact values.

In the expressions for $\frac{\beta(t)}{\alpha_0}$,

$$K_0=\frac{p_0}{E}\left\{\frac{M_\alpha}{I_Y}\frac{N_r}{I_Z}+\frac{L_\alpha}{mV}\left[\frac{M_q}{I_Y}\frac{N_r}{I_Z}+p_0^2\left(\frac{I_Y-I_X}{I_Z}\right)\left(\frac{I_Z-I_X}{I_Y}\right)\right]\right\}$$

$$K_1=\frac{p_0}{(a^2+\omega^2)(C-2\omega^2)}\sqrt{\omega^2\left[-\omega^2-\frac{M_\alpha}{I_Y}+p_0^2\left(\frac{I_Y-I_X}{I_Z}\right)\left(\frac{I_Z-I_X}{I_Y}\right)\right]^2+\left[\frac{M_\alpha}{I_Y}\frac{N_r}{I_Z}+\omega^2\left(-2a+\frac{N_r}{I_Z}+\frac{M_q}{I_Y}\right)+\frac{L_\alpha}{mV}\left(\frac{I_Y-I_X}{I_Z}\right)\left(\frac{I_Z-I_X}{I_Y}\right)p_0^2\right]^2}$$

$$\epsilon=\tan^{-1}\frac{1}{\omega}\frac{-\frac{M_\alpha}{I_Y}\frac{N_r}{I_Z}-\omega^2\left(-2a+\frac{N_r}{I_Z}+\frac{M_q}{I_Y}\right)-\frac{L_\alpha}{mV}\left(\frac{I_Y-I_X}{I_Z}\right)\left(\frac{I_Z-I_X}{I_Y}\right)p_0^2}{\left[-\omega^2-\frac{M_\alpha}{I_Y}+p_0^2\left(\frac{I_Y-I_X}{I_Z}\right)\left(\frac{I_Z-I_X}{I_Y}\right)\right]}$$

$$K_2, K_3, \text{ and } K_5=\frac{p_0\left[\frac{M_\alpha}{I_Y}\left(\frac{N_r}{I_Z}\frac{1}{\lambda}-1\right)+p_0^2\left(\frac{I_Y-I_X}{I_Z}\right)\left(\frac{I_Z-I_X}{I_Y}\right)\left(1+\frac{L_\alpha}{mV}\frac{1}{\lambda}\right)\right]}{2C\lambda+D}$$

$$K_4=\frac{p_0}{D}\left\{\frac{M_\alpha}{I_Y}\frac{N_r}{I_Z}+\frac{L_\alpha}{mV}\left[\frac{M_q}{I_Y}\frac{N_r}{I_Z}+p_0^2\left(\frac{I_Y-I_X}{I_Z}\right)\left(\frac{I_Z-I_X}{I_Y}\right)\right]\right\}$$

In the expressions for $\frac{\Delta\alpha(t)}{\alpha_0}$,

$$K_0=-\frac{p_0^2}{E}\left[\left(\frac{I_Y-I_X}{I_Z}\right)\left(\frac{I_Z-I_X}{I_Y}\right)p_0^2-\frac{N_\beta}{I_Z}\left(\frac{I_Z-I_X}{I_Y}\right)+\frac{M_q}{I_Y}\frac{N_r}{I_Z}\right]$$

$$K_1=\sqrt{C_2^2+C_1^2}$$

$$K_2, K_3, \text{ and } K_5=-\frac{p_0^2\left[\lambda^2-\left(\frac{M_q}{I_Y}+\frac{N_r}{I_Z}\right)\lambda+p_0^2\left(\frac{I_Y-I_X}{I_Z}\right)\left(\frac{I_Z-I_X}{I_Y}\right)-\frac{N_\beta}{I_Z}\left(\frac{I_Z-I_X}{I_Y}\right)+\frac{M_q}{I_Y}\frac{N_r}{I_Z}\right]}{\lambda\,(2C\lambda+D)}$$

$$K_4=-\frac{p_0^2}{D}\left[\left(\frac{I_Y-I_X}{I_Z}\right)\left(\frac{I_Z-I_X}{I_Y}\right)p_0^2-\frac{N_\beta}{I_Z}\left(\frac{I_Z-I_X}{I_Y}\right)+\frac{M_q}{I_Y}\frac{N_r}{I_Z}\right]$$

$$\epsilon=\tan^{-1}\frac{C_2}{C_1}$$

where

$$C_2=-\frac{p_0^2}{\omega^2\,(C-2\omega^2)}\left[\omega^2+\left(\frac{I_Z-I_X}{I_Y}\right)\frac{N_\beta}{I_Z}-p_0^2\left(\frac{I_Z-I_X}{I_Y}\right)\left(\frac{I_Y-I_X}{I_Z}\right)\right]$$

$$C_1=-C_2\left(\frac{a}{\omega}\right)-\frac{2a-p_0^2\left(\frac{M_q}{I_Y}+\frac{N_r}{I_Z}\right)}{\omega\,(C-2\omega^2)}$$

The C, D, and E appearing in the preceding expressions are the coefficients of the characteristic equation. A comparison of the motions obtained by using the exact and approximate coefficients is shown in figures 2 to 4 to be very good.

EFFECT OF ASSUMING p_0 CONSTANT AT $t=0$

In general, the rolling velocity builds up exponentially in response to an aileron input instead of being constant at $t=0$ as assumed in this analysis. In order to determine the effect of the assumption on the motions in β and $\Delta\alpha$, an analog study was conducted with the assumption that the rolling velocity reaches its steady-state value exponentially. The resultant motions in β and $\Delta\alpha$ were compared with the

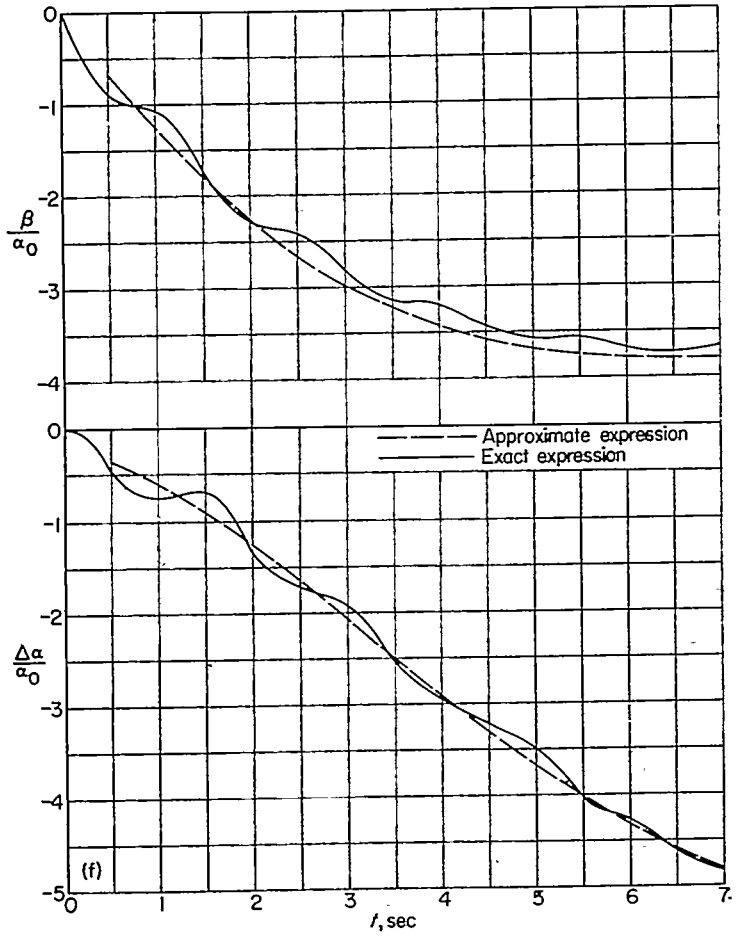

(f) $p_0=-2.5$.

FIGURE 3.—Continued.

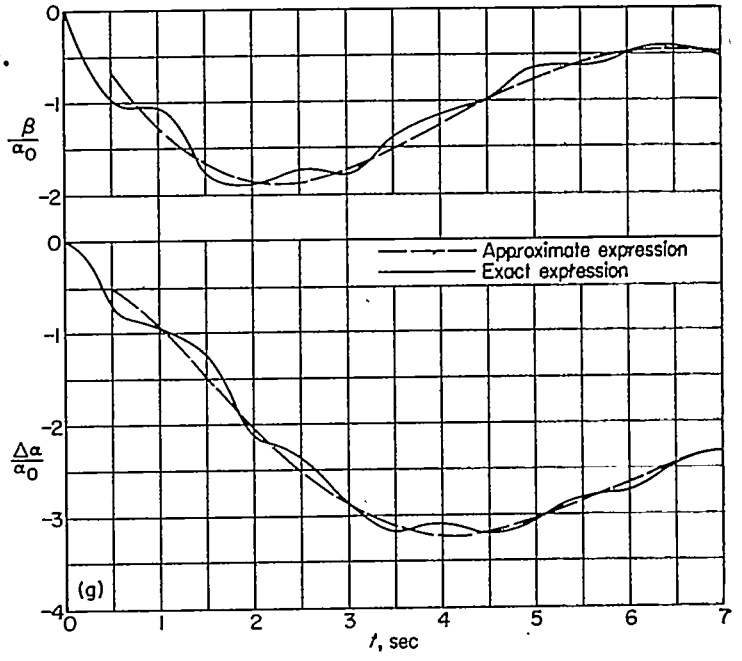

(g) $p_0=-3.0$.

FIGURE 3.—Concluded.

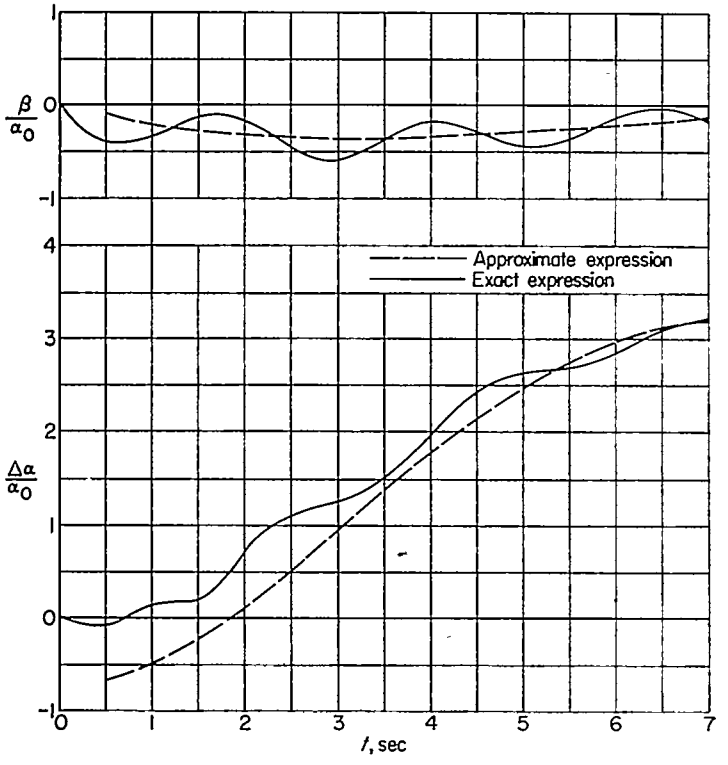

FIGURE 4.—Time histories of β/α_0 and $\Delta\alpha/\alpha_0$ for $C_{m_\alpha}=-0.09$, $C_{n_\beta}=0.114$, $p_0=-1.0$, and $C_{Y_\beta}=C_{L_\alpha}=0$.

motions in β and $\Delta\alpha$ obtained on the assumption that p_0 is constant at $t=0$. Equations (1) were used in the analog study and, in addition, a simplified roll equation $\dot{p}-\frac{qSb^2}{2VI_x}C_{l_p}p=\frac{M_x}{I_x}$ was introduced. This equation states that p reaches its steady-state value, p_0, according to the expression $p=p_0(e^{\lambda t}-1)$. In general, the resultant motions obtained in the analog study were very similar to the motions shown in figures 2 and 3. The only significant difference noted was that different peak values of $\frac{\Delta\alpha}{\alpha_0}$ and $\frac{\beta}{\alpha_0}$ were encountered. Table III presents a comparison between the maximum values of $\frac{\Delta\alpha}{\alpha_0}$ and $\frac{\beta}{\alpha_0}$ obtained from the analog study and from figures 2 and 3 for $p_0=-1.0$, -1.5, and -3.0. It is seen from the values presented in table III that higher maximum values occur for $p_0=-1.0$ and -1.5 for the condition of constant p_0 at $t=0$ whereas the opposite is true for $p_0=-3.0$. These results can be explained by the fact that, during the first several seconds of the transient motion, the average value of p_0 in the analog study is smaller than under the assumption of constant p_0. Hence in the analog study for $p_0=-1.0$ and -1.5 the airplane may be considered to be located farther away from the stability boundary, but for $p_0=-3.0$ the airplane is located closer to the stability boundary.

CALCULATIONS OF MOTIONS FOR AN AIRPLANE PERFORMING A 360° ROLL

The analysis presented thus far is applicable to the condition of the airplane performing a continuous rolling motion. Of particular interest are the motions of the airplane when the pilot performs a 360° roll. These motions can be approximated by first determining the values of β, r, α, and q at the time the airplane has rolled through 360°, that is, at $t=\frac{2\pi}{p_0}$. At this value of t, the constant rolling velocity is returned to $p_0=0$ and the motion originally described by four degrees of freedom is now separable into its lateral and longitudinal values, the former represented by the yawing and sideslipping equations and the latter represented by the pitching-moment and normal-force equations. Thus, the values of β, r, α, and q at $t=\frac{2\pi}{p_0}$ are the initial conditions required to calculate the motions subsequent to $t=\frac{2\pi}{p_0}$. The values of β and α can be determined from equation (3), (4), or (5). From equations (1c) and (1d), the following equations are obtained:

$$r=\frac{Y_\beta}{mV}\beta+p_0\alpha_0+p_0\Delta\alpha-\dot{\beta} \tag{6}$$

and

$$q=\frac{L_\alpha}{mV}\Delta\alpha+p_0\beta+\dot{\alpha} \tag{7}$$

A good approximation of r and q at $t=\frac{2\pi}{p_0}$ is obtained by neglecting the terms $\dot{\beta}$ and $\dot{\alpha}$ in equations (6) and (7). The following table compares the values of r and q at $t=\frac{2\pi}{p_0}$ for $p_0=-1.5$, -1.7, and -3.0 when $\dot{\beta}$ and $\dot{\alpha}$ are included in

TABLE III

COMPARISON OF MAXIMUM VALUES OF $\frac{\beta}{\alpha_0}$ AND $\frac{\Delta\alpha}{\alpha_0}$

p_0	C_{L_α}, C_{Y_β}	$\left(\frac{\beta}{\alpha_0}\right)_{max}$		$\left(\frac{\Delta\alpha}{\alpha_0}\right)_{max}$	
		p_0 constant at $t=0$	$p=p_0(e^{\lambda t}-1)$	p_0 constant at $t=0$	$p=p_0(e^{\lambda t}-1)$
−1.0	0	−0.64	−0.48	0.5	0.4
−1.0	Finite	−.6	−.48	.4	.3
−1.5	0	−1.64	−1.27	1.0	.9
−1.5	Finite	−1.48	−1.12	.68	.6
−3.0	0	−1.75	−1.91	−3.92	−4.15
−3.0	Finite	−1.90	−2.1	−3.25	−3.3

equations (6) and (7) and then deleted from equations (6) and (7):

p_0	$\dot{\beta}$ and $\dot{\alpha}$ included		$\dot{\beta}$ and $\dot{\alpha}$ deleted	
	r	q	r	q
−1.5	−0.20	0.20	−0.19	0.19
−1.7	−.12	.33	−.14	.32
−3.0	.25	.30	.29	.40

EFFECT OF GRAVITY TERMS ON THE β AND $\Delta\alpha$ MOTIONS

The effect of the gravity components which would appear in the side force (eq. (1c)) and normal force (eq. (1d)) equations have been neglected in this analysis. In order to determine the effect of the gravity terms on the β and $\Delta\alpha$ motions, an analog study was conducted using equations (1c) and (1d) with the gravity terms included and then deleted from the equations. The airplane was assumed to be performing a 360° roll for rolling velocities of $p_0=-1.5$, -1.7, and -3.0. A comparison of the maximum values of $\frac{\beta}{\alpha_0}$ and $\frac{\Delta\alpha}{\alpha_0}$ obtained with and without the gravity terms is presented in table IV. The two values given for $\frac{\Delta\alpha}{\alpha_0}$, that is, $\frac{\Delta\alpha_1}{\alpha_0}$ and $\frac{\Delta\alpha_2}{\alpha_0}$, correspond to the maximum values of $\frac{\Delta\alpha}{\alpha_0}$ obtained during the initial part of the transient motion (p_0=constant) and during the recovery part of the motion ($p_0=0$), respectively. The comparison shows that with the gravity terms included the maximum values of β are about 2° greater and the maximum values of $\Delta\alpha$ increase by about 1° for an initial α_0 of 5°.

TABLE IV

COMPARISON OF MAXIMUM VALUES OF $\frac{\beta}{\alpha_0}$ AND $\frac{\Delta\alpha}{\alpha_0}$

p_0	Gravity terms included			Gravity terms deleted		
	$\left(\frac{\beta}{\alpha_0}\right)_{max}$	$\left(\frac{\Delta\alpha_1}{\alpha_0}\right)_{max}$	$\left(\frac{\Delta\alpha_2}{\alpha_0}\right)_{max}$	$\left(\frac{\beta}{\alpha_0}\right)_{max}$	$\left(\frac{\Delta\alpha_1}{\alpha_0}\right)_{max}$	$\left(\frac{\Delta\alpha_2}{\alpha_0}\right)_{max}$
−1.5	−1.8	−0.50	0.90	−1.4	−0.30	0.90
−1.7	−2.5	−.60	1.3	−2.1	−.40	1.2
−3.0	−3.0	−2.4	1.5	−2.7	−2.2	1.6

CONCLUDING REMARKS

From the analysis presented in this paper it appears that the transient motion in angles of attack and sideslip during a constant rolling maneuver consists chiefly of either an oscillatory mode or two aperiodic modes. Approximate expressions are derived for the determination of these modes as well as the modal coefficient corresponding to each mode. Inclusion of the derivatives C_{Y_β} (side force due to sideslip) and C_{L_α} (lift-curve slope) increases the total damping of the system but does not markedly affect the transient motions.

The sole input considered in this paper is the term $p_0\alpha_0$ (the product of rolling velocity and trim angle of attack) in the side-force equation.

LANGLEY AERONAUTICAL LABORATORY,
NATIONAL ADVISORY COMMITTEE FOR AERONAUTICS,
LANGLEY FIELD, VA., *May 22, 1956.*

APPENDIX

METHOD OF APPROXIMATING THE ROOTS OF THE CHARACTERISTIC EQUATION

The fourth-degree characteristic equation

$$A\lambda^4+B\lambda^3+C\lambda^2+D\lambda+E=0$$

may be factored as follows:

$$(\lambda^2+a_1\lambda+b_1)(\lambda^2+a_2\lambda+b_2)=0$$

where

$$A=1$$

$$B=a_1+a_2$$

$$C=b_1+b_2+a_1a_2$$

$$D=a_2b_1+a_1b_2$$

$$E=b_1b_2$$

An examination of the quadratic equations from which the exact roots presented in tables II (a) and II (b) were obtained indicated that $b_1 \gg b_2$ and that a_1 and a_2 are of the same order of magnitude and much smaller than b_1. Thus, one may write

$$A=1$$

$$B=a_1+a_2$$

$$C=b_1$$

$$D=a_2b_1$$

$$E=b_1b_2$$

The solution of these equations yields

$$a_1=\frac{BC-D}{C}$$

$$b_1=C$$

$$a_2=\frac{D}{C}$$

$$b_2=\frac{E}{C}$$

The roots of $\lambda^2+a_1\lambda+b_1=0$ approximate the high-frequency mode whereas the roots of $\lambda^2+a_2\lambda+b_2=0$ approximate the remaining two roots of primary importance in the motion calculations presented herein. A comparison between the exact roots and the approximate roots presented in tables II (a) and II (b) indicates that the agreement is excellent.

REFERENCES

1. Phillips, William H.: Effect of Steady Rolling on Longitudinal and Directional Stability. NACA TN 1627, 1948.
2. Churchill, Ruel V.: Modern Operational Mathematics in Engineering. McGraw-Hill Book Co., Inc., 1944.